Article

Applied Spectroscopy
2018, Vol. 72(6) 943–946

DOI: 10.1177/0003702818762092
journals.sagepub.com/home/asp
SAGE

Design and Fabrication of Far-Ultraviolet Reflective Broadband Filter Based on Dielectric Materials

Xiaodong Wang[1], Bo Chen[1], and Ling Yao[2]

Abstract

In the far-ultraviolet (UV) region, optical materials are dispersive and absorbing. The previous successful design method utilized in the visible band should be re-examined. We report on the design and fabrication of a far-UV reflective broadband filter based on dielectric materials lanthanum fluoride (LaF_3) and magnesium fluoride (MgF_2). Extended bandwidth technology is utilized in designing this filter. The obtained filter has a high reflectance in the working wavelength range of 140–180 nm, meanwhile, with good suppression in shorter and longer wavelength regions. In 2016, this filter was employed in a wide-angle aurora imager (WAAI) installed in the Feng Yun III satellite that will be launched in China.

Keywords

Lanthanum fluoride, LaF_3, magnesium fluoride, MgF_2, broadband, filter

Date received: 14 November 2017; accepted: 5 February 2018

Introduction

The aurora is a global scale phenomenon resulting from collisions between the atmosphere and energetic particles originated from the solar wind. Imaging of the earth's aurora provides valuable, considerable information about solar–terrestrial connection, such as energy flux and characteristics of precipitating particles.[1–4] The N_2 Lyman–Birge–Hopfield (LBH) band at 140–180 nm is one of the widely studied airglow emissions in the far-ultraviolet (UV) range. Far-UV reflective filters selectively reflected emissions in the ranges of 140–160 nm, 160–180 nm, and 140–190 nm, respectively, and suppressed unwanted spectrum. They were developed to guarantee the purity of target lines and meet the requirements of N_2 LBH band imaging.[1–4] A special far-UV reflective broadband filter (RBF) was employed in the far-UV wideband imaging camera installed in the IMAGE spacecraft, and it has the average reflectance of about 60% in the range of 140–190 nm, and an additional visible and near-UV suppression.[4] Unfortunately, they did not provide film materials used in their multilayer. In addition, design strategies for filters are based on the assumption that there is no absorption or optical dispersion of materials, which is valid in the visible region and not in the far-UV region. In the far-UV region, the absorption of materials cannot be ignored and optical dispersion of materials becomes significant, which makes designing far-UV filters complicated. Optical dispersion of materials leads to a reduction in the steepness of edges of a stop band, and absorption of materials results in a decrease of reflectance in a stop band. In addition, in 2017, a wide-angle aurora imager (WAAI) installed in the Feng Yun III satellite will be launched in China. A far-UV RBF that aims at selectively reflecting emission lines in 140–180 nm is in urgent demand in this WAAI. Our group has developed an aluminum–magnesium fluoride (Al/MgF_2) non-periodic multilayer, and it shows a good spectral response. However, the reflectance at 135.6 nm is too high (>10%) and the central wavelength shifts (5 nm) towards the longer waveband after two months.[5]

In this paper, we will design and fabricate a far-UV RBF based on dielectric multilayer, and our filter will have a high reflectance in 140–180 nm and a better suppression in shorter and longer wavelength regions than the previously developed Al/MgF_2 multilayer by our group.[5]

[1]State Key Laboratory of Applied Optics, Changchun Institute of Optics, Fine Mechanics and Physics, Chinese Academy of Sciences, Changchun, China
[2]Shenyang Aircraft Design and Research Institute, Shenyang, China

Corresponding author:
Xiaodong Wang, Dongnan Hu Road 3888#, Changchun, 130033 China.
Email: wangxiaodong@ciomp.ac.cn

Design of the Reflective Broadband Filter

As shown in Eq. 1, the reflectance bandwidth of the quarter-wave (QW) multilayer is determined by the ratio of refractive indices of two materials used in the construction of the stack, where $\Delta\lambda$ is the width of reflectance zone, λ_0 is reference wavelength, and, n_H and n_L are the indices of high- and low-index layers, respectively.[6] The reflectance bandwidth is calculated to be 17 nm using Eq. 1 for the lanthanum fluoride–magnesium fluoride (LaF_3/MgF_2) QW multilayer with a reference wavelength of 160 nm, which is less than half of our target (40 nm). In calculation, the refractive indices of LaF_3 and MgF_2 at 160 nm are 1.795 and 1.518, respectively.

$$\Delta\lambda = \frac{4}{\pi}\sin^{-1}\left(\frac{n_H - n_L}{n_H + n_L}\right)\lambda_0 \quad (1)$$

The optical constants of LaF_3 and MgF_2 are derived from characterization of reflectance (10°, 20° incidence) of the single layer by OptiLayer software.[7] In order to obtain 40 nm of reflectance bandwidth, a method of overlapping of two QW stacks with different central wavelengths in a single coating is utilized to extend the reflectance zone. This process was discussed in detail by Turner and Baumeister,[8] and it has been widely, successfully employed in design and fabrication of visible filters.[9–11] This process was then applied in the far-UV. Two stacks with central wavelengths of 150 nm and 170 nm, respectively, are superposed in a single coating to achieve a filter with a central wavelength of 160 nm for an extended high reflectance zone in the range of 140–180 nm.

Figure 1 shows theoretical reflectance curves of QW stacks of Multilayer A (central wavelength of 150 nm), Multilayer C (central wavelength of 160 nm), Multilayer B (central wavelength of 170 nm), and Multilayer A+B. Due to adsorption of materials, these coatings have a lower reflectance compared to QW coatings (R > 99%) in the visible region. Due to dispersion of materials, these coatings have less steep edges of the stop band and reflectance curves are similar to Gaussian type lines. In contrast, reflectance curves of QW coatings in the visible region are similar to rectangles. The reflectance bandwidths of Multilayers A, B, C, and A+B are 20 nm, 21 nm, 24 nm, and 36 nm, respectively. It should be noted that the reflectance bandwidth calculated by Eq. 1 differs from the one derived from Fig. 1. This is because optical dispersion of film materials in the far-UV is ignored in calculating reflectance bandwidth by Eq. 1. Multilayer A+B has an extended reflectance zone and meets our design goal. The first layer near the substrate is LaF_3 and the last layer near air is MgF_2. However, there are two valleys (oscillation) in the reflectance zone due to lower steepness of

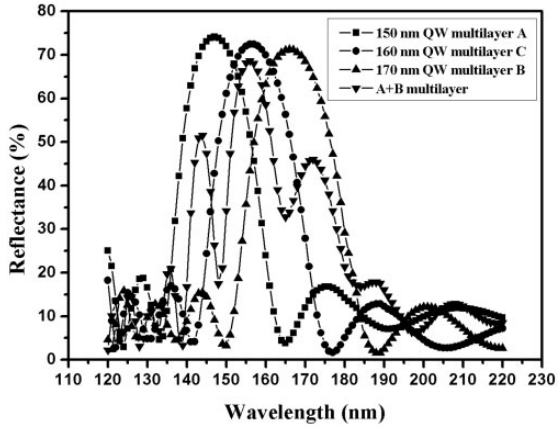

Figure 1. Theoretical reflectance curves of 13-layer QW stacks with the central wavelength of 150 nm, 160 nm, and 170 nm, respectively, and 26-layer Multilayer A+B (Multilayers A and B are superposed in a single coating). The incident angle is 22°.

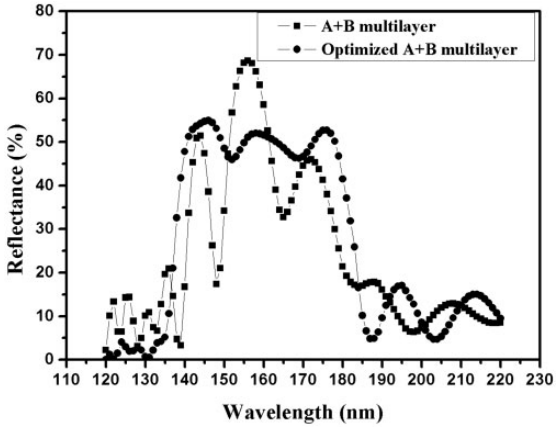

Figure 2. Theoretical reflectance curves of Multilayer A+B and optimized Multilayer A+B. The A+B multilayer was further optimized using OptiLayer software.[7]

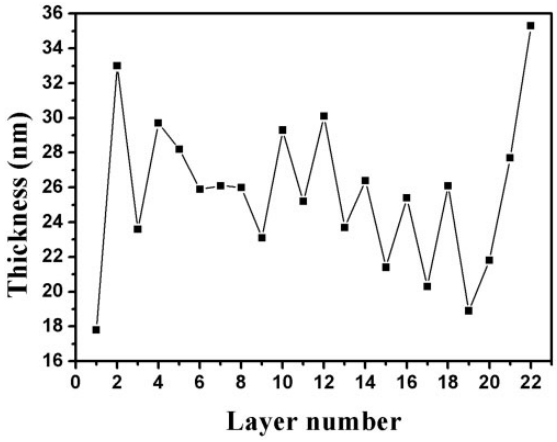

Figure 3. Thickness distribution of the optimized multilayer.

Multilayers A and B, and there are ripples out of the reflectance band. Thus, Multilayer A+B still needs further optimization.

In order to reduce the oscillation in the reflectance zone and suppress the reflectance out of the stop band, the target reflectance is reduced from 70% to 50%, which is a compromise we must make between reflectance and uniformity. Theoretical reflectance curves of Multilayer A±B and optimized Multilayer A±B are presented in Fig. 2. The optimized A±B multilayer has a better reflectance zone, a good reflectance suppression in 120-137 nm, and no improvement in 181-220 nm, which meets our requirement. The average reflectance is 50.0% in 140-180 nm, 3.8% in 120-137 nm, and 12.6% in 181-220 nm. The reflectance bandwidth is 44 nm. Figure 3 demonstrates thickness distribution of optimized multilayer and the first layer is near the substrate.

Fabrication of Reflective Broadband Filter

The used LaF_3 and MgF_2 have a purity of 99.99%. The depositions were made in a thermal evaporation vacuum system. The base pressure was 3.0×10^{-4} Pa. LaF_3 was evaporated by heated resistance boat and MgF_2 in the copper crucible was evaporated by electron beam. The voltage of the electron gun was fixed at 10 kV, the thickness of films and deposition rate were controlled using a quartz crystal (IC6, Inficon Company). The distance between the source and substrate was 50 cm; the distance between the quartz crystal and source was 45 cm. The deposition rate of LaF_3 and MgF_2 was 0.5 nm/s. The fused silica substrate was heated to 250° before deposition.

The reflectance and transmittance of films in the wavelength range of 120–130 nm were measured by our own developed spectrophotometer with a step of 1 nm, and the base pressure was 2.0×10^{-4} Pa. The reflectance and transmittance of films in the wavelength range of 131–380 nm were measured by McPherson VUVaS 2000 ultraviolet spectrophotometer with a step of 1 nm, and the base pressure was 4.0×10^{-3} Pa. The reflectance of films in the wavelength range of 381–760 nm was characterized by a Lambda 1050 ultraviolet–visible–near-infrared (UV-Vis-NIR) spectrophotometer with a step of 1 nm in the ambient atmosphere.

Experimental Results

Figure 4 indicates reflectance curves of theoretical design and experiment for 26-layer optimized Multilayer A+B. The incident angle is 22°, which is the working angle of this filter. The experimental reflectance curve has a relatively good agreement with the theoretical one. The average reflectance is 49.9% in 140–180 nm, 6.7% in 120–137 nm, and 12.5% in 181–220 nm. The reflectance bandwidth is 44 nm.

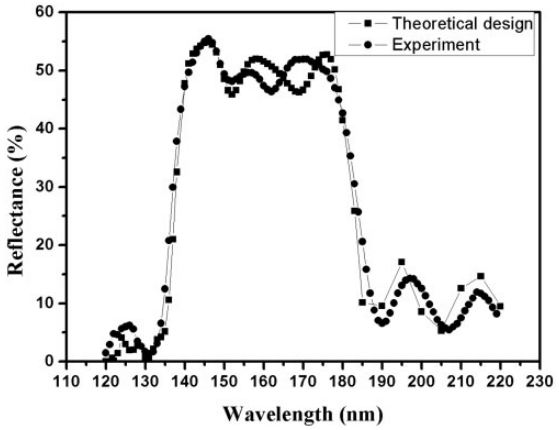

Figure 4. Reflectance curves of theoretical design and experiment for the 26-layer optimized Multilayer A+B.

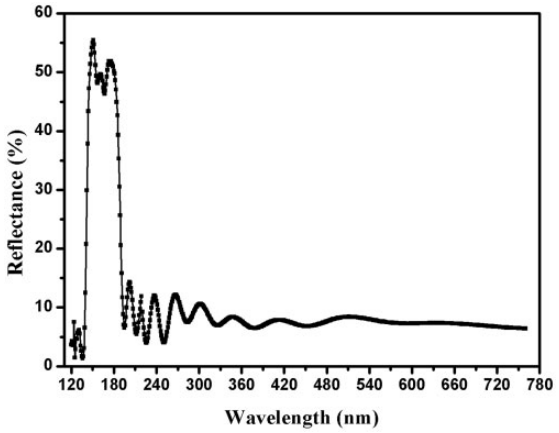

Figure 5. Experimental reflectance curve of 26-layer far-UV RBF in 120–760 nm. The incident angle is 6°.

Figure 5 demonstrates experimental reflectance curve of 26-layer far-UV RBF in 120–760 nm. The incident angle is 6°. The mean reflectance is 7.6% in 221–760 nm, which indicates that obtained RBF has excellent reflectance suppression in the UV and visible regions.

It should be noted that if more layers are added, better spectral performance could be obtained. However, more added layers results in an increase of accumulated film thicknesses, which makes multilayers crack. It is experimentally found that it is free of cracking when the total thickness is < 700 nm under our deposition condition, and there is still no cracking on the surface of multilayer when the multilayer undergoes strong UV radiation and high-, low-temperature environment. Figure 6 indicates two- and three-dimensional pictures of a cracked 32-layer LaF_3/MgF_2 non-periodic multilayer and the accumulated thickness of the 32-layer coating is 756 nm. This phenomenon

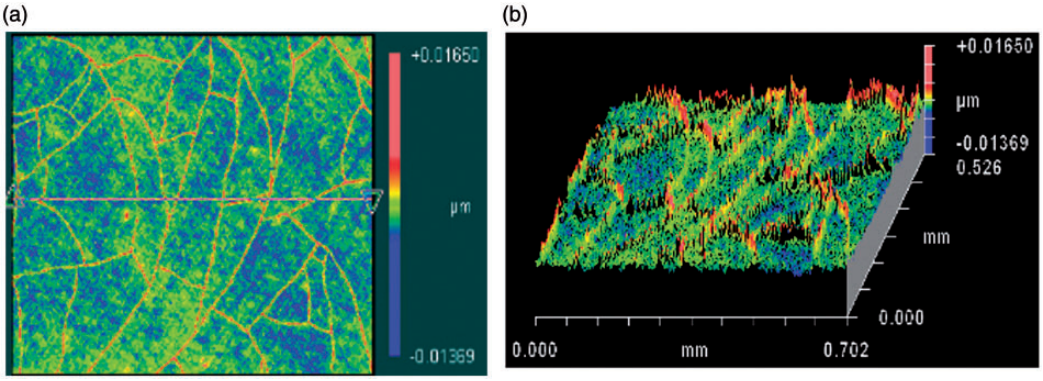

Figure 6. (a) Two- and (b) three-dimensional images of cracked 32-layer LaF_3/MgF_2 non-periodic multilayer.

results from high values of thermal stress of LaF_3 and MgF_2,[12,13] especially MgF_2.

Conclusion

Although materials in the far-UV are dispersive and absorbing, traditional extending reflectance band methods in the visible band are still effective in the far-UV, but modern computer software should be employed to further optimize initial designed multilayers. A far-UV RBF was designed by a traditional method of combining two QW stacks with different central wavelength into a single coating. This RBF was successfully fabricated by thermal evaporation method and has been utilized in a WAAI installed in the Feng Yun III satellite.

Acknowledgments

We thank Professor Alexander Tikhonravov from Moscow State University for his fruitful discussions of the characterization of the optical constant of MgF_2 films.

Conflict of Interest

The authors report there are no conflicts of interest.

Funding

This work is partially supported by the Joint Research Fund in Astronomy (U1531106, U1731114) under cooperative agreement between the National Natural Science Foundation of China (NSFC) and Chinese Academy of Science (CAS).

References

1. M. Zukic, D.G. Torr, J. Kim, J.F. Spann, et al. "Filters for the International Solar Terrestrial Physics Mission Far-Ultraviolet Imager". Opt. Eng. 1993. 32(12): 3069–3074.
2. M.R. Torr, D.G. Torr, M. Zukic, R.B. Johnson, et al. "A Far Ultraviolet Imager for the International Solar–Terrestrial Physics Mission". Space Sci. Rev. 1995. 71(1–4): 329–383.
3. M. Zukic, D.G. Torr. "Multiple Reflectors as Narrow-Band and Broadband Vacuum Ultraviolet Filters". Appl. Opt. 1992. 31(10): 1588–1596.
4. S.B. Mende, H. Heetderks, H.U. Frey, M. Lampton, et al. "Far Ultraviolet Imaging from the Image Spacecraft. 2. Wideband FUV Imaging". Space Sci. Rev. 2000. 91(1–2): 271–285.
5. X.D. Wang, B. Chen, H.F. Wang, F. He, et al. "Design and Fabrication of Far Ultraviolet Filters Based on π-Multilayer Technology in High-κ Materials". Sci. Rep. 2015. 5: 8503.
6. H.A. MacLeod. "Thin-Film Optical Filters". Boca Raton, FL: CRC Press, Taylor and Francis, 2010. 4th ed.
7. A.V. Tikhonravov, M.K. Trubetskov. "Optilayer Thin Film Software". http://www.optilayer.com [accessed Jan 08 2017].
8. A.F. Turner, P.W. Baumeister. "Multilayer Mirrors with High Reflectance Over an Extended Spectral Region". Appl. Opt. 1966. 5: 69–76.
9. K.V. Popov, J.A. Dobrowolski, A.V. Tikhonravov, B.T. Sullivan. "Broadband High-Reflection Multilayer Coatings at Oblique Angles of Incidence". Appl. Opt. 1997. 36(10): 2139–2151.
10. M.-M. de Denus-Baillargeon, T. Schmitt, S. Larouche, L. Martinu. "Design and Fabrication of Stress-Compensated Optical Coatings: Fabry–Perot Filters for Astronomical Applications". Appl. Opt. 2014. 53(12): 2616–2624.
11. K.N. Chopra, K.V. Narasimham. "Thin Film Coating Design and Fabrication of Broadband Dielectric Coated Laser Mirror". J. Opt. 1986. 17(2): 107.
12. M.-C. Liu, C.-C. Lee, M. Kaneko, K. Nakahira, et al. "Influence of Ion Assistance on LaF_3 Films Deposited by Molybdenum Boat Evaporation". Appl. Opt. 2012. 51(15): 2865–2869.
13. M.-C. Liu, C.-C. Lee, M. Kaneko, K. Nakahira, et al. "Microstructure-Related Properties at 193 Nm of MgF_2 and GdF_3 Films Deposited by a Resistive-Heating Boat". Appl. Opt. 2006. 45(7): 1368–1374.